Towards a Numerical Model for the Rate of Heat Evolution in Concrete Based on Binder Chemistry and w/c Ratio

Y. Ballim[1], P.C. Graham, C.J. Greensmith
University of the Witwatersrand, Johannesburg, South Africa

Abstract
Designing against the potential for thermally induced cracking in concrete structures requires a reliable assessment of the time-temperature profiles that will develop in the concrete. This requires an accurate measure of the reaction-time rate of heat evolution as basic input information. This paper presents the development and experimental assessment of a heat rate model that includes parameters such as the w/c ratio, chemistry and crystallography of the cement. The early-age heat rates of a range of concretes were measured in an adiabatic calorimeter and these were used to train the numerical model. Based on comparative experimental work to date, the model seems to predict heat rates reliably. Nevertheless, the model will have to be assessed and further refined against a broader range of measured heat rates before it can be reliably used for temperature prediction in concrete structures.

Keywords: cement, hydration, heat, adiabatic, maturity, concrete.

1 Introduction
Designing against the potential for thermally induced cracking in mass concrete structures requires an accurate assessment of the time-temperature profiles that are likely to develop in the concrete. This is usually achieved through a solution of the Fourier equation for heat flow using a numerical technique involving time and space increments. Whatever the nature of such an analysis is, the solution requires a reliable measure of the time-based rate of heat evolution during the hydration reactions as basic input information.

A number of empirical approaches have been developed to provide a measure the rate of heat evolution as a function of time. These have taken the form of rough, generalised values of total heat liberated over the early period of hydration for different binder types [1] or cement components [2] or guide equations for the rate of heat evolution [3]. Ballim and Graham [4] have presented a criticism of these approaches to heat rate modelling, particularly because many of them rely on a fixed maximum heat rate. Furthermore, where a maturity approach is included, this is based on a

[1] Private Bag 3, WITS, 2050. yunus.ballim@wits.ac.za

cumulative maturity which is unable to account for changes in the rate of hydration as a result of changes absolute temperature.

Alternatively, the rate of heat evolution can be directly measured using techniques such as adiabatic or isothermal calorimetry. However, both these approaches are limited in their use value, particularly because experience has shown that large variations in the heat rate profile are possible with cementitious materials that are nominally considered to be similar. A rigorous approach which is based on direct measurement of the heat-rate profile will therefore require that each cement binder be tested to provide input for a temperature prediction estimate. There is clearly a need for a model of the rate of heat evolution of cement which is based on the chemistry, composition and morphology of the cementitious binder used.

In the present study, the multi-component heat rate model proposed by Kishi, et al [5] and more completely presented by Maekawa et al [6], was modified and refined in response to observed heat rate characteristics of a range of cements tested. The model incorporates parameters such as the chemistry, crystallography and fineness of the cement as well as the presence of cement extenders such as fly ash or ground granulated blast furnace slag and the water content of the mixture. The revised model was assessed by comparison with measured heat rates of six cements prepared in the laboratory. Cement clinker was collected from six different manufacturing facilities and these were prepared into cements so that the processing variables remained the same. The cements were then used to prepare concretes for adiabatic testing. A separate cement sample was also used to assess the effects of water:cement ratio (w/c) on the measured heat rates. These results were used to propose further modifications to the model.

The paper also presents an argument for expressing such models in terms of maturity-based heat rates rather than time-based heat rates. This is also a more suitable form of the heat rate function for use in a numerical solution of the Fourier equation for temperature prediction in concrete elements.

2 Brief Description of the Heat Rate Model

The model presented here is essentially based on the principle of superposition in that it assumes that the total heat produced during cement hydration is the sum of the heats produced by the individual crystallographic compounds participating in the reactions. The idea that Portland cement hydration can be analysed on the basis on the individual hydration reactions of the constituent phases has been commented on by a number of authors [7,8]. Steinhour [8] found “a degree of agreement to

support the assumption that the clinker compounds react essentially independently". While the principle of superposition is a reasonable first assumption in this application, Van Breugel [9] correctly cautions that the possibility of interaction between components during hydration requires further investigation.

The form of the model assessed and further developed in this study is as presented by Maekawa, et al [6]. The final equations governing the operation of the model are presented here while Section 3 presents details of the modifications that were made to model to improve the form and quality of prediction.

The rate of heat released by hydrating Portland cement, H_c, is given by:

$$H_c = \sum p_i H_i$$
$$= p_{C_3A}(H_{C_3AET} + H_{C_3A}) + p_{C_4AF}\left(H_{C_4AFET} + H_{C_4AF}\right) + p_{C_3S}H_{C_3S} + p_{C_2S}H_{C_2S} \qquad (1)$$

where:

H_{C_3AET} and H_{C_4AFET} are the heat release rates when ettringite is formed in the reactions of C_3A and C_4AF with gypsum and p_i and H_i are weight composition ratio and the heat liberation rate for the i^{th} mineral component respectively. The weight composition ratio is determined from a Bogue analysis of the cement [10].

H_i is determined from Equation 2 below.

$$H_i = \beta_i s_i \mu H_{i,T_0}(Q_i)\exp\left\{-\frac{E}{R}\left(\frac{1}{T}-\frac{1}{T_0}\right)\right\} \qquad (2)$$

For simplification, this equation only includes those parameters pertinent to the hydration of Portland cement on its own without mineral extenders or other admixtures and:

β_i is a coefficient representing the reduction of heat liberation rate due to the reduced availability of free water and precipitation space.

s_i is a coefficient that changes the heat rate in accordance with the fineness of the powder.

μ is a coefficient that expresses the changes in the heat liberation rate due to the changing mineral composition of the Portland cement.

H_{i,T_0} is the reference heat liberation rate of component i at constant temperature T_0 and is a function of the accumulated heat Q_i.

$$Q_i \equiv \int H_i dt \qquad (3)$$

$$\beta_i = 1 - \exp\left\{-5\left[\left(\frac{w_{free}}{100\cdot\eta_i}\right)s_i^{(0.5)}\right]^{2.4}\right\} \qquad (4)$$

In Equation 4: $w_{free} = \frac{W_{total} - \sum W_i}{C}$ (5)

The coefficient, h_i, which represents the thickness of the internal reaction layer is calculated from the expression:

$$h_i = 1 - \left(1 - \frac{Q_i}{Q_{i,\infty}}\right)^{\frac{1}{3}} \quad (6)$$

W_{total} and W_i are the total water content at mixing and the updated values of the water consumed by each component as hydration progresses. $Q_{i,\infty}$ is the total heat liberated at the completion of each hydration reaction and Q_i is the accumulated heat liberated by the i^{th} component up to point of hydration under consideration.

The rates of heat liberation, (H_{i,T_0}), that arise from the individual component hydration exothermic reactions are determined from data developed by Maekawa et al [6]. Also, the model assumes that after the cement grains come into contact with water, chemical reactions occur in the following sequence:

- Formation of ettringite from C_3A
- Formation of ettringite from C_4AF
- Simultaneous hydration of C_3A, C_4AF, C_3S and C_2S

In addition, it is assumed that approximately one-third of the C_3A and one percent of the C_4AF is consumed in the formation of ettringite.

3 Proposed Modifications to the Model

3.1 Maturity form of the heat rate function

The model was developed to operate in a commercially available spreadsheet and used to predict the heat rate profiles of cements with differing phase compositions. An important modification was to express the resulting heat rates in terms of maturity rather than in accumulated hydration heat form. This expresses the time axis in equivalent maturity form or equivalent hydration time at 20 ^oC (t_{20} hours). Also, the heat rate is expressed in units of “joules per maturity second” or “maturity Watts”. Ballim and Graham [4] have shown the importance of this approach as a means of normalising the heat rate function in order to account for differing time-temperature history profiles across a concrete element. This expresses the maturity heat rate (H_M) as:

$$H_M = \frac{dQ_t}{dM} \quad (7)$$

Q_t is the total accumulated heat and M (measured in t_{20} hours) is the Arrhenius maturity defined as:

$$M = \sum_{i=1}^{i=n} \exp\left[\left(\frac{E}{R}\right)\left(\frac{1}{293} - \frac{1}{273 + 0.5.\left(T_i + T_{i-1}\right)}\right)\right] \cdot \left(t_i - t_{i-1}\right) \quad (8)$$

Where, M is the equivalent maturity time (in t_{20} hours); E is the activation energy parameter; R is the universal gas constant (8.314 J/mol.^{o}C); T_i is the temperature (^{o}C) at the end of the i^{th} time interval, t_i. The value of E was taken as a constant (= 33.5 kJ/mol [11]) as suggested by Bamford and Tipper [12].

The time-based heat rate is then determined using the chain rule as follows:

$$H_t = H_M \frac{dM}{dt} \quad (9)$$

This means that numerical models aimed at predicting time-temperature profiles in concrete structures, should correctly be structured to monitor both the maturity as well as the rate of change of maturity at different locations within the concrete element.

3.2 Duration of ettringite formation

In the model, ettringite is allowed to form for approximately 0.6 t_{20} hours and the normal cement hydrations commence thereafter. Using this timing it was found that the peak heat was reached earlier than observed in practice. To compensate for this, a period of 2 t_{20} hours was added to the calculated time values from the end of the ettringite reactions. Besides correcting the time to reach the peak heat rate, the addition of 2 t_{20} hours creates a dormant period in the heat rate profile, which is often observed.

3.3 Peak heat rate profile

Equation 3 results in a steep single point heat rate peak of short duration that is not normally encountered in experimental results. This was adjusted by adding a further 2 t_{20} hours to all of the time data occurring after the peak heat rate is reached. This intervention results in a flat peak that is not truly representative of the hydration heat release rates but was considered close enough to provide a reasonable estimate.

3.4 Post peak heat rate profile

After the peak heat rate has been reached, the rate of heat liberation progressively diminishes until it reaches a very low rate and continues to release heat at this low rate for a considerable time. The application of the coefficient, β_i, as formulated by Maekawa et al [6] results in a sharp decline in heat rate that differs considerably from the experimental results. For this reason it was decided to represent the declining portion of the heat rate profile using the expression:

$$H_C = H_{C,\max} \cdot \exp\left[-0.04\left(t_{20,i} - t_{20,H_{\max}}\right)\right] \quad (10)$$

Where:
H_C = the sum of the heat rates liberated by all of the components
$H_{C,max}$ = the maximum heat rate attained
$t_{20,H_{\max}}$ = the maturity time in t_{20} hours at the end of the period of maximum heat release
$t_{20,i}$ = maturity time at the i^{th} time interval.

4 Experimental Assessment of the Model

4.1 Assessment of the adjusted model

Six cement clinker samples were drawn from the production plants belonging to three cement companies operating in South Africa. Each of these production plants manufacture Type 1 cement which satisfies the requirements of the local standard specification, SABS ENV 197 [13]. To ensure that the samples were representative of current production, each clinker was drawn from the moving stock just before entry into the grinding mill. Approximately 3.5 kg of clinker was drawn from each plant and this was used to manufacture cement in the laboratory. Table 1 shows the results of the X-ray fluorescence analysis of the clinkers.

Table 1: Results of XRF analysis of the clinker samples.

	% Composition of clinker					
	A	B	C	D	E	F
CaO	66.50	65.57	67.60	65.6	68.40	65.06
SiO_2	22.30	22.15	22.80	21.90	22.10	22.26
Fe_2O_3	3.61	2.98	1.90	1.57	4.26	3.05
Al_2O_3	3.80	4.51	4.30	5.00	3.80	3.98
MgO	1.10	2.64	1.40	3.70	0.50	2.04
TiO_2	0.18	0.45	0.28	0.26	0.19	0.25
Mn_2O_3	0.05	0.22	0.24	0.72	0.09	0.99
K_2O	0.62	0.16	0.58	0.32	0.39	0.53
Na_2O	0.37	0.20	0.06	0.11	0.19	0.14
SO_3	0.82	0.26	0.27	0.48	0.20	0.21
P_2O_5	0.15	0.00	0.03	0.10	0.16	0.00
Free Lime	1.02	0.80	1.57	0.35	0.82	0.97
LOI	0.80	0.00	0.98	0.16	0.64	0.90
TOTAL	100.2	99.1	100.4	99.9	100.8	99.4

In manufacturing the cements in the laboratory, a sample of gypsum was obtained from one of the production plants and, based on a chemical analysis of the gypsum and the clinkers, the amount of gypsum added to each of the clinkers was adjusted so that each cement had an SO_3

content of 2.3%. The same gypsum type and SO_3 content was used to ensure that the rate of heat evolution of each clinker was compared on the basis of clinker characteristics only. Also, while an SO_3 content of 2.3% is typical of South African cements, in reality, manufacturers would adjust the SO_3 content in response variations to aspects such as the C_3A content of the clinker.

Each clinker with the appropriate amount of gypsum was ground in a laboratory ball mill. The mill was periodically stopped and the specific area of the sample was determined using a Blaine apparatus. Grinding was stopped when the measured specific surface area of the sample was 3200 $\pm$ 50 cm^2/g. Using this procedure, the average fineness measured for the six samples was 3198 cm^2/g with a standard deviation of 24 cm^2/g.

4.2 Effects of w/c ratio

In a second phase of the investigation, a fresh sample of commercially produced cement was obtained from one of the manufacturing plants with a view to assessing the effects of changes to w/c ratio on the heat rate profile. The intention was to provide an independent basis for further adjustment of the model to account for variations in the w/c ratio. Table 2 shows the chemical composition of the cement for this part of the study.

Table 2: Chemical composition (%) of cement used for w/c ratio adjustment tests

CaO	SiO_2	Al_2O_3	Fe_2O_3	MgO	SO_3	TiO_3	Mn_2O_3	P_2O_5	LOI
65.9	22.6	3.6	2.4	3.1	2.6	0.3	0.9	0.1	1.8

4.3 Adiabatic calorimeter testing

Each of the cements prepared from the clinkers shown in Table 1 was used to prepare a concrete for testing in an adiabatic calorimeter as described by Gibbon, et al [14]. For this series of tests, the mixture proportions of the concrete test sample are shown in Table 3. This mixture yields sufficient material to produce a 1.2 litre sample of concrete.

Table 3: Mixture composition of the concrete used for the adiabatic calorimeter tests

Laboratory cement	420 g
9.5 mm washed silica stone	1020 g
Graded, washed silica sand	1060 g
Water	280 mℓ

To assess the effects of w/c ratio, the cement described in Table 2 was used to prepare three concretes with w/c ratios of 0.4, 0.5 and 0.6 which were then tested in the adiabatic calorimeter. The mixture proportions for this series of tests are shown in Table 4.

Table 4: Mixture proportions of the concretes used for assessing the effects of w/c ratio on adiabatic calorimeter tests

w/c ratio	0.4	0.5	0.6
Cement (g)	757	606	505
9.5 mm silica stone (g)	1240	1240	1240
Silica sand (g)	1088	1214	1297
Water (mℓ)	303	303	303

4 Results and Discussion

Figure 1 shows the results of the adiabatic heat rate measurements on the six laboratory prepared cements compared with the heat rates predicted by the adjusted model (note that the heat rates are presented in maturity form, as discussed above). This figure shows that the model provides a reasonable approximation of the heat rates for cements A, B, C, E and F. In the case of cement A and, to a lesser extent, cement E, the model predicts the time to peak heat rate as occurring approximately 5 t_{20} hours earlier than was observed. The prediction of the time to peak heat rate is fairly good in the case of cements B, C and F.

Not all the cements showed the period of sustained heat rate level at the peak heat rate. This means that the inclusion of a 4 t_{20} hour dormant period in the model may have to be revised. However, the crystallographic or cement composition reason for the presence or absence of this sustained heat rate level is not clear and will require further investigation.

The model prediction of the declining limb of the heat rate curves is also fairly good. However, the measured results for cements B, C and (perhaps) E show characteristic “shoulder” peaks in the declining limb of the heat rate curves. This is usually identified as the conversion of ettringite to monosulphate hydrate. The model, including our proposed revisions, is clearly not able to reproduce this feature of the hydration of the cements. In this context, an added complication is the fact that not all the cements tested showed this ettringite conversion shoulder. Here again, it would be necessary to provide a cement compositional basis to explain these differences before a further refinement of this aspect of the model can be undertaken.

Cement D stands out as showing particularly poor correlation between the measured and predicted heat rates. This measured heat rate profile was reproduced upon re-resting and a sample of the commercially produced cement from this plant showed a similar heat rate profile after testing in the adiabatic calorimeter. The model predicts the first part of the ascending limb and the later part of the descending limb of the curve fairly well. However, the model predicts a peak heat rate of approximately 2 W/kg whereas the measured value was approximately 4.6 W/kg. It is clear

that there are crystallographic, morphological or compositional features of this cement which are not adequately accounted for by the model. Ballim and Graham [15] have shown that this level of inaccuracy in estimating the peak heat rate of the cement can result in significant error in the estimation of the time-temperature profile of large concrete structures.

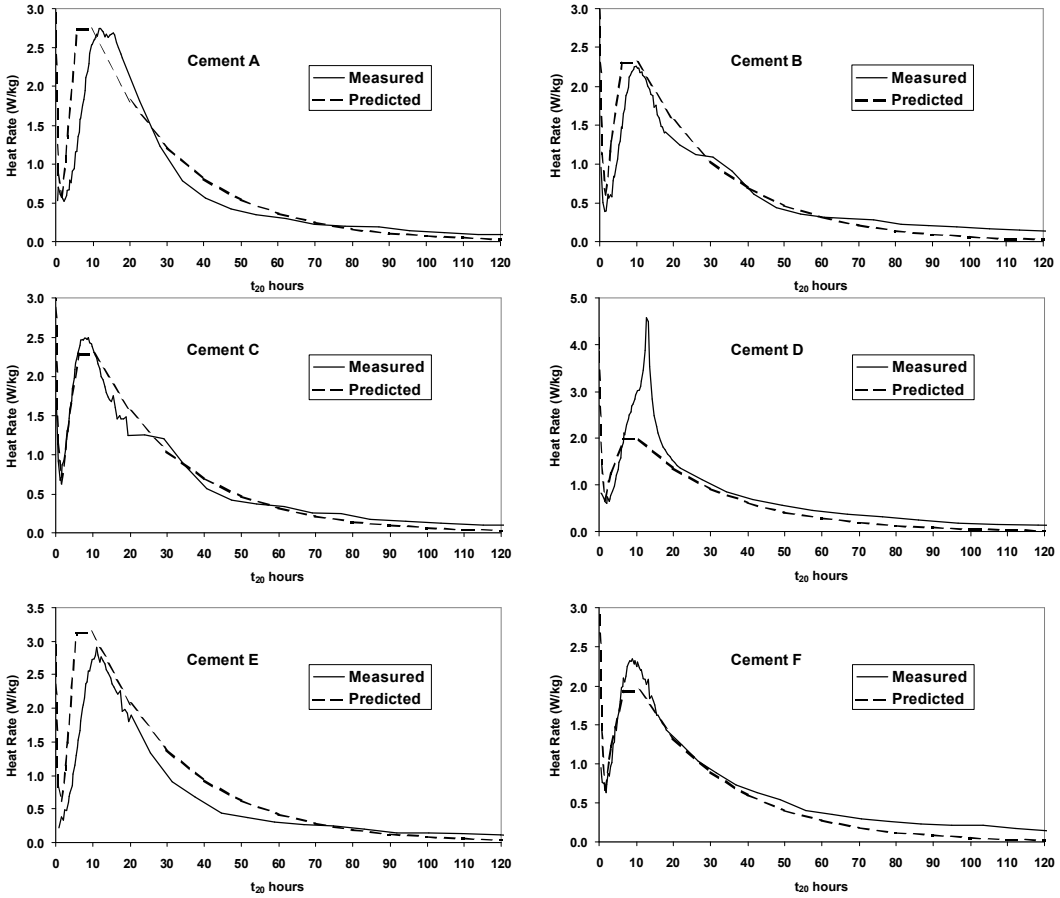

Figure 1: Modelled and experimental heat rate curves for the six laboratory cements assessed

Reference to Table 1 shows that Cement D has the highest Al_2O_3 and MgO contents of the cements tested. This also translates to the highest alumina ratio and calculated C_3A content. If this is the reason for the unusual peak heat rate profile, the model, as presently structured, does not adequately account for this feature of cement chemistry and crystallographic composition. It is likely that an explanation is to be found in the combined interaction of the Al and Mg compounds.

Adjustments for w/c ratio

The results of the adiabatic calorimeter tests on the concrete mixtures presented in Table 4 were used to develop adjustments to the model to account for the effects of w/c ratio. In essence, these adjustments aim to

account for differences in the accessibility of the mix water to the hydration needs of the cement.

The coefficient β_i from Equation 2, was further adjusted (β_{iadj}),as shown in Equation 11. The experimental coefficient, c_i, in Equation 11 is determined for the hydration of the various cement phases, ettringite formation and monosulphate conversion processes, from Equation 12 and Table 5.

$$b_{iadj} = b_i \left(\frac{0.6}{w/c} \right)^{c_i} \quad (11)$$

$$c_i = A_c \cdot \ln(w/c) + B_c \quad (12)$$

Table 5: Empirical values of A_c and B_c for use in Equation 12.

	C_3S	C_2S	C_3A	C_4AF	Ettringite	Mono-sulphate
A_c	-2.949	-2.941	-2.952	-2.941	1.475	1.475
B_c	0.265	-0.162	0.106	-0.012	6.642	1.842

The reaction start times (t_{0i}) for the various hydration phases and hydration processes were also adjusted in response to variations in the w/c ratio. This was done on the basis of the empirically determined Equation 13 and Table 6.

$$t_{0i} = A_t \cdot \ln(w/c) + B_t \quad (13)$$

Table 6: Empirical values of A_t and B_t for use in Equation 13.

	C_3S	C_2S	C_3A	C_4AF	Mono-sulphate
A_t	3.933	3.941	4.424	4.441	4.424
B_t	8.080	11.402	9.727	10.772	15.277

Finally, Equation 14 was developed based on the results of this series of tests to adjust the duration (t_3) of the main hydration rate peak (peak 3) in response to variations in the w/c ratio.

$$t_3 = 4.305 \cdot \ln(w/c) + 6.426 \quad (14)$$

Figure 2 shows the effects of including the proposed w/c ratio adjustments into the model, in relation to the results from which the adjustments were empirically derived. To illustrate the effect, only the results of the 0.6 and 0.4 w/c ratio tests are shown here. The 0.5 w/c ratio concrete gave results that were similar to those of the 0.4 concrete. The results show that the adjustments are more suitable for application to the lower w/c ratio concretes and may not be appropriate at higher w/c ratio levels. There is clearly a need for further work in this area, which must include the effects

of a range of concrete mixture design issues such as admixtures, concrete workability and cement fineness.

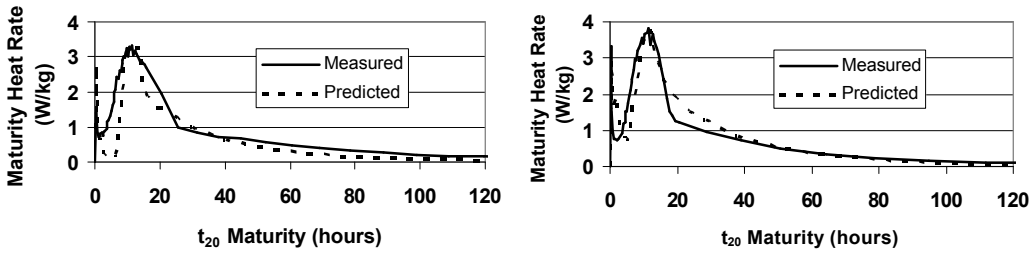

Figure 2: Heat rate curves predicted with the w/c ratio adjustment for concretes with w/c ratios of (a) 0.6 and (b) 0.4

5 Conclusions

As described and with the proposed modification implemented, the model provides an adequate approximation of the heat rate profiles of five of the six cements tested. However, notwithstanding the relatively small error, the model is unable to correctly describe the shape of the peak heat rate profile. Also, where it occurs, the model does not reproduce the "shoulder" on the declining limb of the heat rate curve caused by the conversion of ettringite to monosulphate hydrate.

The model is also particularly unable to adequately describe the peak heat rate profile of cement D. At this stage, it appears that this is caused by the inability of the model to correctly account for the influence of the aluminate phases and, in particular, the C_3A component in modifying the heat rate characteristics of cement.

The test results indicate that the w/c ratio of concrete has an important influence in modifying the measured heat rate profile of concrete. It is likely that this is a feature of both the access to water by the hydrating cement, as well as the rate of temperature increase in the initial stages of hydration. While the proposed modifications to the model to account for the effects of variations in w/c ratio look promising, further refinements are clearly necessary, particularly at the higher w/c ratio levels.

Finally, the results point to the direction in which further work in this area should be aimed. This is essentially towards a better and deeper understanding of the chemical and morphological effects of cement on the nature and kinetics of hydration.

6. References

[1] Addis, BJ (ed.). Fulton's concrete technology (6th Revised Edition). Portland Cement Institute, Midrand, South Africa. 1986.

[2] Scanlon, J. M. and McDonlad, J. E. Thermal properties, in: Kleiger, P. and Lamond, J. F. (eds), Significance of tests and properties of concrete and concrete-making materials, ASTM-STP 169C. American Society for Testing and Materials, Philadelphia, 1994, Chapter 24, pp 229-239.
[3] Wang, C.H and Dilger, W.H. Prediction of temperature distribution in hardening concrete, in: Springenschmid, R (ed.), Thermal Cracking in Concrete at Early Ages. E&FN Spon, London, 1994, pp. 21-28
[4] Ballim, Y and Graham, PC. A maturity approach to the rate of heat evolution in concrete, Magazine of Concrete Research. 55 (3) (2003) 249-256
[5] Kishi, T, Shimomura, T and Maekawa, K. Thermal crack control of high performance concrete, in RK Dhir and RM Jones (Eds.), Concrete 2000, Economic and durable construction through excellence. E&FN Spon, London, 1999, pp. 447-456.
[6] Maekawa, K, Chaube, R and Kishi, T. Modelling of Concrete Performance – Hydration, Microstructure Formation and Mass Transport, Routledge, London, 1999.
[7] Copeland, L.E., Kantro, D. L., and Verbeck, G., Chemistry of Hydration of Portland Cement, in: Fourth International Symposium on the Chemistry of Cement, U. S. Department of Commerce, Washington, 1962.
[8] Steinhour, H.H, The Reactions and Thermocheistry of Cement Hydration at Ordinary Temperature, in: Third International Symposium on the Chemistry of Cement, Cement and Concrete Association, 1952.
[9] Van Breugel, K, Numerical Simulation of Hydration and Microstructural Development in Hardening Cement Based Materials, Heron. 37 (2) 1992, Delft University of Technology, Delft
[10] Lawrence C.D. The constitution and specification of Portland cements, in: Hewlett PC (Editor). Lea's Chemistry of Cement and Concrete, 4th Edition. London, Arnold. 1988. Chapter 4.
[11] CEB-FIP, Model Code for Concrete Structures, Comite Euro-International du Beton, Lausanne, Switzerland, 1990.
[12] Bamford, C. H. and Tipper, C. F. H. (eds.) Comprehensive chemical kinetics, Vol. 1: The practice of kinetics. Elsevier Publishing Company, London, 1969.
[13] SABS ENV 197-1:2000. Cement – Part 1: Composition, specifications and conformity criteria for common cements. South African Bureau of Standards, Pretoria, 2000
[14] Gibbon G.J, Ballim Y and Grieve G.R.H. A low-cost, computer-controlled adiabatic calorimeter for determining the heat of hydration of concrete. ASTM Journal of Testing and Evaluation, 25 (2) (1997) 261-266
[15] Ballim, Y and Graham, P.C. Early-age heat evolution of clinker cements in relation to microstructure and composition: implications for temperature development in large concrete elements. Cement and Concrete Composites, 26 (2004), 417-426